RSC Advances

ROYAL SOCIETY OF CHEMISTRY

www.rsc.org/advances

RSC Advances

RSCPublishing

ARTICLE

Nano Bio Optically Tunable Composite Nanocrystalline Cellulose Films

Cite this: DOI:

Y. Nevo[a†], N. Peer[b†], S. Yochelis[b], M. Igbaria[c], S. Meirovitch[c], O. Shoseyov[a]* and Y. Paltiel[b]*

Received ooth ,
Accepted ooth

DOI:

www.rsc.org/

Plastic pollution creates major environmental damages especially when taking into account the constant increase in plastic films use. Therefore, increasing the use of biodegradable films and reducing non degradable plastic usage is a worldwide necessity. Current biodegradable films are not transparent or strong enough for most applications. In this work we utilize nanocellulose and semiconductor nanocrystals to reinforce and functionalize a biodegradable transparent film to create a transparent, strong and optically tunable plastic film. Nanocrystalline cellulose is produced from cellulose fibers, the main component of the plant cell walls. The nanocrystalline cellulose particles are 5–20 nm in diameter, a few hundreds of nanometers in length, and have superb mechanical properties. The optical properties are controlled by introducing nanocrystals within the nanocellulose layers. The hybrid nanocellulose / nanocrystals films reinforcement will enable the reduction in the amount of the plastic polymer in most polymeric articles while maintaining mechanical integrity with additional optical properties.

[a] The Robert H. Smith Institute of Plant Sciences and Genetics in Agriculture, The Hebrew University of Jerusalem, Rehovot 7610001, Israel.

[b] Department of Applied Physics, The Hebrew University of Jerusalem, Givat Ram, Jerusalem 9190401, Israel

[c] Valentis Nanotech Ltd. Industrial zone, Misgav 2017900, Israel.

† The first two authors contributed equally to the work

Introduction

The routine and extensive use of plastic films composed of such materials as polyethylene (PE), polyethylene terephthalate (PET) and polypropylene (PP) has greatly increased, becoming a major environmental concern. The ability to reduce the amounts of such polymers in polymeric articles while maintaining mechanical integrity and endowing the materials with optical properties, has thus far been proved unsuccessful. In this work we utilize nanocryslalline cellulose (NCC) and semiconductor nanocrystals (NCs) unique characteristics to produce transparent strong films with tunable optical properties. These reinforced films can reduce the thickness of needed non-degradable PE PET or PP, or it can enhance the properties of degradable films, such as poly(lactic acid) (PLA).

NCC, produced by hydrolysis of cellulose fibers has attracted a lot of attention due to its physical, chemical and mechanical properties. A variety of cellulose sources can be used in order to produce NCC, such as cotton,[1] wood,[2] bacterial cellulose,[3,4] microcrystalline cellulose (MCC),[5] and even recycled wood pulp, which is present in waste streams of paper mills and municipal sewage system sludge. The use of sulfuric acid in the hydrolysis process results in rod-shaped nanoparticles, which are negatively charged due to the formation of sulphate ester groups on their surface, leading to a well dispersed and stable water suspension. Above a certain critical concentration, the NCC suspension can form ordered liquid crystal phases.[6] The advantages of NCC, namely its superb properties, renewability, biodegradability and abundance, lead to its recognition as one of the most promising materials for future applications. NCC is nearly as strong as Kevlar and can be added to materials to increase their strength and stiffness.[7–10] Many studies in recent years have shown that NCC can be used as a building block in a variety of applications. The most common use of NCC is as filler in nanocomposite materials[11–13] but it has also been utilized in other applications such as adhesives,[14,15] foams, aerogels [16,17] and films [18–20].

Upon drying, NCC liquid crystal water suspension is known to self-assemble into macro scale ordered films, as seen in fig. 1a.

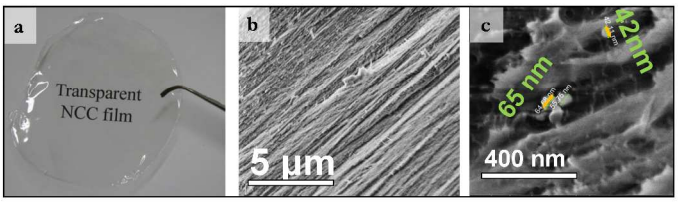

Fig. 1 (a) Dried NCC film. (b) SEM micrograph of an independent NCC film prepared with ZnO NCs. (c) Zoomed SEM micrograph of an independent NCC film prepared with ZnO NCs. note the ZnO NCs located between the layered

NCC films can be transparent or semitranslucent and can retain the liquid crystalline order of the suspension.[21] Furthermore, NCC-based films and composite material were found to have good gas barrier properties, attributed mainly to the high crystallinity of the nano crystals which lower the diffusion of gas molecules and elongate the path they travel through the film.[22] Alone or combined with other materials, self-assembled NCC films with intriguing properties enable cost effective, tunable coatings for large surfaces.

Quantum dots are quantum confined structures in all three dimensions.[23] Consequently, electrons and holes occupy discrete energy states. Furthermore electrons in quantum dots buried in a quantum well may tunnel from one dot to the next. This gives rise to delocalization effects and to the creation of minibands which are of considerable scientific interest.[24] These unique quantum properties have attracted in recent years a great deal of scientific and technological interest. From the applications point of view quantum dots allow the use of quantum mechanics in the real world of ambient temperature operating devices. Such devices include optoelectronic,[25,26] quantum information processing[27,28] and energy harvesting devices.[29,30] In particular semiconductor quantum dots have a large potential for applications in optoelectronics.[31]

Semiconductors quantum dots, referred in this article as semiconductor nanocrystals (NCs), are emerging as useful building blocks of electro-optical devices, due to their size, composition and shape dependent photoluminescence.[32,33] using the same NCS and changing their size will create optical tunability of the absorption. For example, InAs-based NCs are tunable in the near-infrared (NIR), effectively covering the telecom range. In recent years simple cheap methods were developed to fabricate highly efficient quantum dots.[34,35] An appealing feature of such colloidal systems is the chemical accessibility allowing flexible processing. InAs and PbS NCs light-emitting diodes operating in the NIR were embedded within a semiconductor polymer matrix.[36–38] InAs colloidal dots were also incorporated in waveguide structures[33] and evidence for optical gain has recently been reported.[32] The chemical accessibility of the colloidal NCs also enables to link them to different surfaces.[39] Moreover, efficient emission has been reported for CdSe dots deposited on surfaces of quantum wells, introducing an additional attractive method for electrical activation of their fluorescence.[40] Recently, it has been demonstrated that the electronic properties of semiconductor-based devices can be modified by organic molecules adsorbed on their surfaces.[41] Therefore, the combination of organic molecules and NCs can further enhance the ability to control properties of the hybrid system.

In the presented work we have combined the NCC properties with the NCs to fabricate strong, optically controlled, biodegradable films that have the potential for many applications such as green houses and food packaging. We have used thin self-assembled layers of NCC to trap NCs inside the NCC films. The NCs can be well dispersed within NCC films, as seen in fig. 1c. For both greenhouses and packaging applications the optical tunability of the absorption spectrum as well as mechanical reinforcement and gas barrier properties are needed. For food packaging it is critical to prevent UV light transmission in order to prevent the peptides denaturation[42] and photo oxidation of essential oils.[43] In greenhouses UV can reduce insect parasites navigation capabilities [44] and infrared absorption enhances the efficiency of the greenhouse.[45,46]

Methods

The fabrication process includes three stages: (a) The NCC was produced by acid hydrolysis of the amorphous weak parts of cellulose fibers. After the hydrolysis we wash the acid and finally, we use sonication in order to get a homogeneous, clear solution of NCC. (b) The NCs solution was mixed with the NCC solution in different ratios and finally (c), it was dried upon a plastic petri dish or plastic film - PE, biaxially oriented polypropylene (BOPP) and PET.

NCC production was based on the method of Pranger and Tannenbaum. Micro Crystalline Cellulose (MCC, Avicel®, FMC Biopolymer Inc.) was hydrolized in 63 wt% H_2SO_4 at a temperature of 60°C with stirring, for 2 hours. Following the hydrolysis, the suspension was centrifuged at 10000 rpm for 10 min. Acid was removed and the pellet was resuspended in deionized water (DIW). The washing and resuspension cycles were repeated for 4 to 5 times until the supernatant coming out of the centrifuge was turbid and the pH of the supernatant was approximately 2. Following the final wash the suspension was dialyzed against DIW for 2 weeks. After dialysis, the suspension was neutralized using NaOH followed by sonication treatment [CL4 ultrasonic convertor, Misonix] that lead to a clear NCC suspension.

At the second stage, we prepared the NCs solutions. We used ZnO Ag doped NCs (M K Impex Corp, ZnO (70 nm) doped with silver, 50 wt% in H_2O, colloidal dispersion) in order to absorb the UV light. ZnO has a wide band gap of 3.37 ev which means it absorbs light with wavelengths lower than 370 nm.[47] Ag doping of ZnO allows a tunable redshift of the NCs due to the shrinkage of the band gap energy.[48,49] Furthermore, ZnO NCs were found to be biocompatible and biodegradable[50]. The ZnO Ag doped NCs solution was further diluted in H_2O in the ratio of 1:500. We also used SiO_2 NCs (Meliorum Technologies SiO_2-H_2O, 5 nm PPS, 50 mg/ 30 ml) in order to block the long wave infrared spectra emitted at room temperature from the greenhouse ground. In this way we could mimic the optical properties of glass and enable better energy conservation of the greenhouse, while maintaining the film flexibility. SiO_2 NCs are also known to be biocompatible and biodegradable.[5152] The SiO_2 NCs solution was further diluted in H_2O in the ratio of 1:100. In order to absorb UV light and emit it in the visible spectra, we used photo-luminescent CdSe/ZnS core-shell quantum dots (QD)s (MKnano, CdSe/ZnS-WS-Yellow stabilized by mercaptoundecanoic acid in H_2O, emission peak 570-585 nm, 25 mg/ 5 ml). The NCs solution was further diluted in H_2O in the ratio of 1:5.

Finally, in the third stage, solutions of mixed NCC and NCs were prepared by mixing the NCs and NCC in varying ratios. The mixed solutions were then used either to achieve NCC based films only, or for coating of thin non-degradable plastic films. In order to produce NCC based films, NCC/NCs solution was dried on a plastic petri dish (see fig. 1a). The diameter of the drops was 1-2 cm and their thickness was to be 50 µm. In order to coat plastic films (PE, BOPP and PET) with NCC suspension, plastic films were first pretreated using N_2-Plasma [PICO UHP plasma system, Diener electronics] which makes the surface of the film positively charged. Coating of plastic films was conducted using a roll coater [K control coater, Printcoat instruments]. NCC suspensions (2 wt%), with or without NCs, were coated upon the surface of the plastic films at a desired wet thickness of 100 µm and was then left to dry.

The resulted dry coating layers were ~1 µm thick. The thickness of the plastic films was 70 µm, 18 µm and 13 µm for PE, BOPP and PET, respectively. The adhesion of the coating layers to the films was tested using the adhesion tape testing method, in which a pressure sensitive tape was used to determine the adhesion quality of the coatings. This test is commonly used in industry.

The prepared samples were then optically measured in the visible spectra by illuminating them with a deuterium/halogen light source (Avantes Avalight-DH-S-BAL) and measuring the transmission with a visible-NIR spectrometer (Ocean Optics USB4000). FTIR measurements were also performed to determine the transmission and absorption in the infrared spectra (Bruker VERTEX-80V). These measurements were performed in vacuum conditions in order to eliminate atmospheric moisture absorptions. The mechanical properties of the films were investigated in both the linear and non-linear range, using an Instron machine (Instron 3345 Tester, Instron, Norwood, MA) equipped with a 100 N load cell. Samples were cut according to ASTM method D882-02 and the thickness was measured using a Mitutoyo Digimatic Indicator (Type ID-S112MB; Mitutoyo Manufacturing Co. Ltd., Tokyo, Japan) at five random posi

For the measurer dye molecule m blue color is trar reduced methylene blue, using 0.8 g NaOH with 15 ml H_2O and 0.5 g of glucose as the reducing agent. After stirring the mixture until the solids were dissolved we added the methylene blue (0.05 g of methylene blue in 50 cm^3 ethanol). The resulting blue solution was reduced after one minute turning to orange. Under nitrogen environment we then gradually mixed agar into the solution until it became a gel. For the experiment we prepared several vials with pierced caps and under the nitrogen environment filled them with the reduced gel. We then covered some of the vials with NCC coated PET films, some with PET and some without a blocking layer as a reference. The vials were then capped with the pierced caps and taken out to room conditions.

Further measurements of the oxygen transmission rate (OTR) of the films were performed on NCC coated BOPP films, using the OX-TRAN® Model 2/21 instrument accordance with ASTM D 3985 under 23°C and 0% RH.

Results

To demonstrate the change in mechanical properties of the new NCC and NCC/NCs coated films, tensile tests experiments were carried out. In these experiments we measured the elastic modulus, tensile stress at break, and tensile strain at break of PE, BOPP and PET films, without any treatment, after plasma pretreatment and after NCC coating (with and without NCs). As can be seen in Table 1, the elastic modulus of PE films coated with NCC increased by more than 100% in comparison to uncoated PE films.

Film	Elastic modulus (MPa)	Stress at break (MPa)	Strain at break (%)
PE	194±10	23±1	1031±41
PE plasma	228±7	23±1	953±32
PE/NCC	414±55	22±1	961±28
PE/NCC/ZnO (1:160)	351±26	22±1	941±16
BOPP	1898±100	104±17	152±10
BOPP plasma	1645±115	100±10	148±10
BOPP/NCC	2377±274	103±10	144±10
PET	4173±190	150±6	94±9
PET plasma	4082±121	150±23	102±7
PET/NCC	4757±221	141±11	92±11

Table. 1 Mechanical properties of coated and uncoated plastic sheets. (n=10, mean±SD)

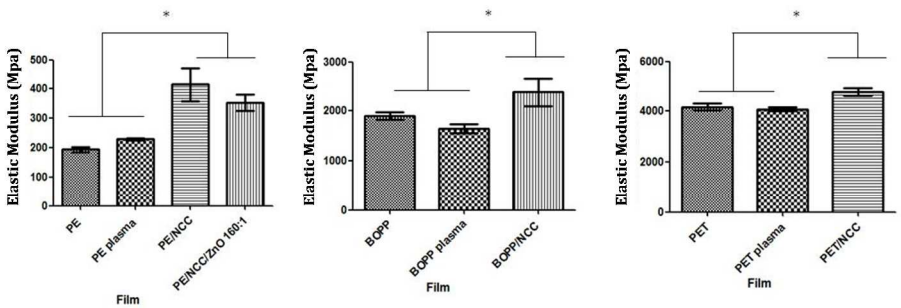

Fig. 2 Elastic modulus of the different plastic sheets. Elastic modulus comparison of coated and uncoated plastic sheets. (* represents statistically significant difference, as analyzed using one way ANOVA for multiple comparison and 2-sample t-test, $p<0.05$)

Furthermore, we found that the addition of NCs to the NCC coat did not compromise the mechanical properties improvement. Both the stress at break and tensile strain at break did not change significantly compared to the uncoated films.

A significant increase of about 20% in the elastic modulus was also observed for coated BOPP films. Due to the very high elastic modulus of BOPP films, the increase was not as dramatic as with PE films.

The elastic modulus of stiff PET films was also improved by the NCC coating, by about 14%. Similar to the coated PE films, the tensile stress at break and tensile strain at break of coated BOPP and PET films did not change significantly.

To test the adhesion of the coatings to the film's surface, we used the adhesion tape testing method. In this experiment no adhesion failure was detected. The BOPP samples with painted NCC coating proved to strongly adhere to the film, without leaving remains of the NCC coating on the tape after being pulled.

Fig. 2 summarizes the statistically significant elastic modulus enhancement of PE, BOPP and PET coated films. In the case of PE films, adding a 1 µm NCC coating to the 70 µm thick PE film was enough to greatly enhance the elastic modulus of the film. For BOPP and PET films, dry NCC layers of 1 µm thickness, coated films of 18 µm and 13 µm, respectively.

A 25 µm thick, biodegradable Poly(lactic acid) (PLA) film was also coated with NCC, resulting in an increase of 65% in elastic modulus compared to uncoated film (data not shown).
As mentioned above NCs possess interesting size-dependent structural, and optical properties.[53] The ability to control the colloidal NCs growth allows one to control the structure, composition, size, and shell structure.[54] Therefore, the actual absorption spectrum of the material can be tuned using quantum
effects. We used this ability to demonstrate the control over optical transmission spectra of the NCC/NCs films, while maintaining mechanical strength of the films.
This is possible as NCs are ordered between the NCC layers as seen in fig. 1c For application use we mainly aimed to demonstrate strong biodegradable films that transmit in the visible while blocking UV and/or mid to far wave infrared spectra (MWIR to LWIR).

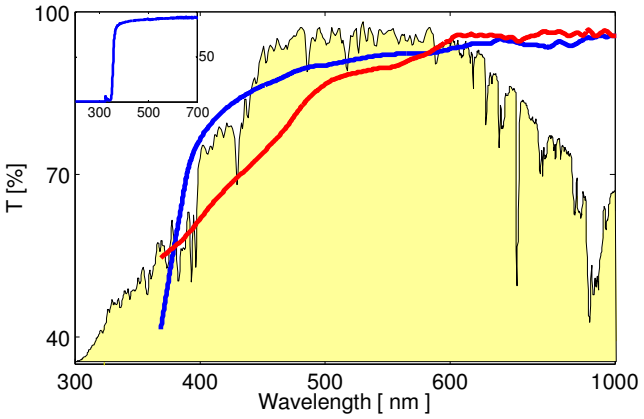

Fig. 3 UV blocking films. Transition plot in the UV and visible spectrum of NCC prepared with ZnO·Ag NCs(blue) at the particle ration of 1:160 ZnO:NCC, NCC prepared with CdSe/ZnS QDs at the particle ratio of 1:50 CdSe:NCC (red). The scaled AM 1.5 solar spectrum is also plotted (yellow). The inset shows the transmission plot of NCC/ZnO coated BOPP film.

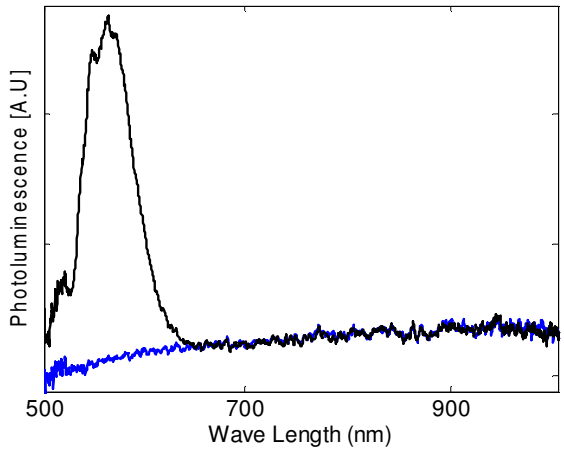

Fig. 4 UV to visible conversion films; Photoluminescence plot of NCC prepared with CdSe/ZnS QDs at the particle ratio of 1:50 CdSe:NCC, illuminated with a 405nm laser (black) compared to the background halogen light (blue).

Blocking UV spectrum enables better protection of crops from insects[44] and also prevents harmful UV exposure for stored food products. Blocking the far IR spectra allows a greenhouse to be more energy efficient by conserving thermal energy within the greenhouse. Around room temperature (300K) most of the block body radiation is concentrated in 4-12 μm range. In this range the glass (SiO_2) absorption efficiency is high while standard polyethylene (PE) is mostly transparent (See fig. 5a). Having a flexible film with glass like absorption properties is an important goal to achieve, thus improving the greenhouse efficiency in a fundamental way.

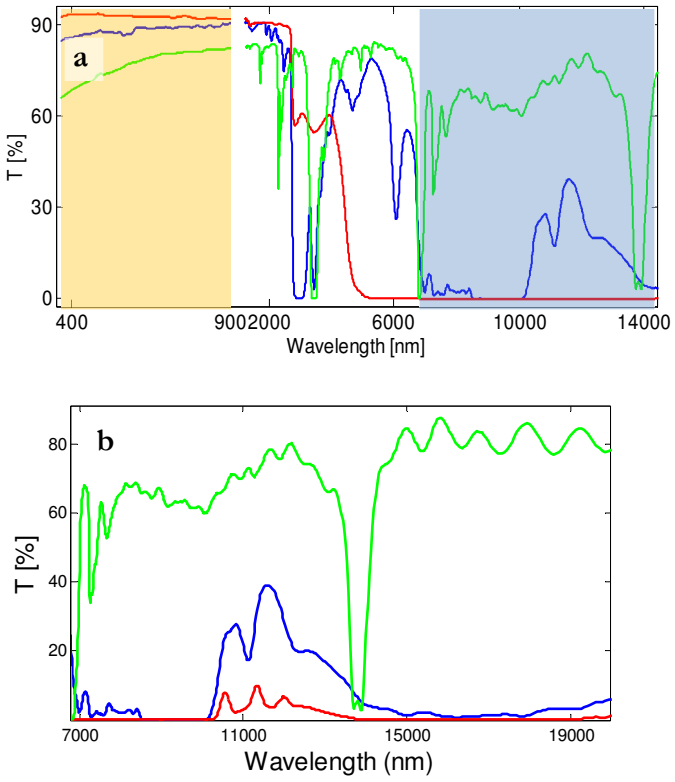

Fig. 5 Glass like NCC films; (a) Visible and IR transmission spectrum of Glass (red), PE (green) and NCC (blue) before any modifications. (b) IR light transmission spectrum of Polyethylene greenhouse films (green) compared to NCC (blue) and NCC prepared with SiO_2 NCs at the particle ratio of 1:150,000 SiO_2: NCC

Fig. 3 shows a control of the absorption of the UV. The films prepared with ZnO•Ag NCs (at the optimal particle ratio of 1:160 ZnO:NCC) displayed a good absorption of light in the UV range (<400 nm) while being almost transparent in the visible range. The ZnO has the band gap of 3.3ev,[55] that creates an absorption peak at 375 nm. Doping the ZnO with silver has shown a band-gap reduction compared to un-doped ZnO, thus creating a red-shift in its absorption.[56] The NCC with CdSe/ZnS core-shell NCs (at the optimal particle ratio of 1:50 CdSe:NCC) shows also good absorption in the UV range with less than 50% transmission at wavelengths lower than 400 nm, without

affecting the transparency in visible light (see fig. 3). This is due to the band gap of the QDs which is 2.14ev as measured by the photoluminescence. Furthermore, in fig. 4 the photoluminescence of CdSe/ZnO QDs is observed, while illuminating the film with a 405nm laser, with an emission peak in the visible range at 570 nm. This demonstrates the ability to convert absorbed UV light to the visible spectra, thus enhancing the greenhouse's efficiency.

Fig. 5a is showing the visible and IR transmission spectrum of a glass, PE and NCC before modification. It is apparent that the PE, as other plastic films, is almost transparent in the visible and IR spectrum. However, while being transparent at the visible the glass has a complete cutoff around 5µm so that the entire MWIR and LWIR spectrum is absorbed. The NCC also shows better absorption than PE in the IR spectrum. The far infrared transmission spectrum of PE films and NCC films mixed with SiO_2 is shown in fig. 5b. The NCC and NCC/ SiO_2 (at the optimal particle ratio of 1:150,000) films were 50µm in thickness while the PE films were 85 µm. It can be seen that NCC shows good IR absorption. This is attributed to the typical cellulosic compounds that are assigned to C-O and C-C ring structures with absorption bands at 8.6 and 9.5 µm.[57]Another absorption band at 11 µm rises from C-O-C stretching (at the β-(1→4) glycosidic linkages) [58]. Other external deformational vibrations of C-H, C-OH, C-CO and C-CH also add to these absorption bands.[57] The NCC with SiO_2 has the most effective absorbance in the IR range relevant for room temperature thermal emission. Thus we achieve the glass like absorption properties in flexible films. This may be due to the absorption bands of SiO_2 (typically asymmetric stretching vibration Si-O-Si bridges (9.0-9.5 µm), and the symmetric vibration stretching of the Si-O-Si bridge (~12.5 µm)) . [59]

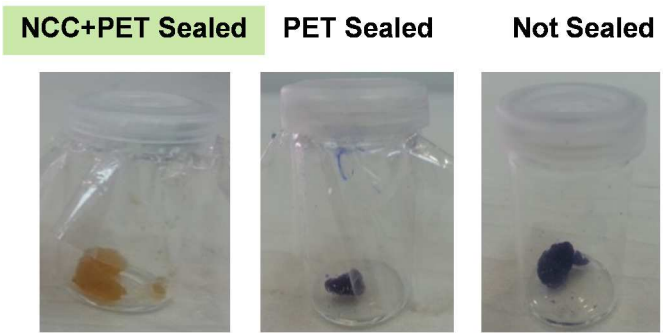

Fig. 6 Oxidation experiment with the color dye of methylene blue after 24 hours under room conditions with pierced caps. The methylene blue gel remained un-oxidized when covered with PET+NCC. When covered with PET or not covered the methylene blue oxidized.

Lastly the same films also acts as oxygen barrier as seen in figure 6. This is extremely important for food packaging where preventing gas flow through the package is crucial. In many standard food packages additional Aluminum foils are added to prevent the oxidation and gas flow. This layer may be removed by using our films. We used the reduced dye molecule methylene blue that acts as an indicator for oxidation. The dye was placed in vials with pierced caps that were covered with the NCC+PET films. We demonstrate that the reduced methylene blue in the vial covered with the NCC+PET (polyethylene terephthalate) layer does not change its color compared to the reference vials with PET only or uncovered dye. In figure 6 we see the vials after 24 hours in room conditions. The dye in the NCC+PET capped vials remained orange while the other references changed their color to blue, meaning the reduced dye was oxidized while the NCC+PET was enough to protect from it oxidation.

Further measurements of the oxygen permeability of the films were performed on NCC coated BOPP films, in which the oxygen transmission rates were measured for 24 hours. The permeability of standard 20μm BOPP films without coating is $2000\frac{cc}{m^2}\ per\ day$. The results of coated BOPP films achieved a rate of less than $1\frac{cc}{m^2}\ per\ day$, showing a significant improvement of the film's oxygen transmission rate. For NCC coated BOPP films the measured rate was $0.64\frac{cc}{m^2}\ per\ day$. Results for NCC/ZnO coated BOPP films were $0.22\frac{cc}{m^2}\ per\ day$, thus showing that the NCs do not compromise the oxygen barrier qualities of NCC but even improve them. The efficient oxygen barrier qualities are within industrial standard for most food packaging applications.

Conclusions

In this work we utilized nanocrystalline celloluse unique properties to produce a biodegradable transparent film with additional controlled optical properties. The film's optical properties were controlled by introducing nanocrystals dispersed within the NCC layers. Following coating of plastic films with NCC, the mechanical properties of plastic films significantly improved, without being compromised by the nanocrystals addition. We showed that we increase the films modulus without reducing the stress or strain. By choosing the optimal plastic film we can achieve flexible sheet properties. These will be used to optimise the impact strength and puncture resistance for packages. We estimate that for all plastic films polymer reduction can be achieved. PE is the weakest film and therefore the largest reduction of around 30% of film thickness is expected. For BOPP and PET films reduction of 10-20% of the plastic polymer used is expected.

In future applications, NCC/NCs hybrid coatings can be used to strengthen polymers, thereby reducing the costs of materials and transport and minimizing their environmental impact, adding tunable optical and other desirable properties.

Author Information

Corresponding Authors

***Y.Paltiel,** Department of Applied Physics, The Hebrew University of Jerusalem, Givat Ram, Jerusalem 91904, Israel**.** paltiel@mail.huji.ac.il

***O. Shoseyov**, The Robert H. Smith Institute of Plant Sciences and Genetics in Agriculture, The Hebrew University of Jerusalem, Rehovot 76100, Israel. shoseyov@agri.huji.ac.il

Author Contributions

The students that have done the experimental part and analyzed the data are the first two authors Y. Nevo and N. Peer. They were helped by Dr. S.Yochelis from Paltiel Lab and Mr. M. Igbaria and Dr. S. Meirovich from Valentis Nanotech. O. Shosayov and Y. Paltiel supervised the work. All authors wrote the paper jointly.

Acknowledgements

O. Shoseyov and Y. Paltiel want to acknowledge the Israel National Nanotechnology Initiative (INNI), Focal Technology Areas program and the HUJI center for nano science and nano technology.

Abbreviations

PE polyethylene,PC polycarbonate, BOPP Biaxially oriented polypropylene, NCC nanocrystalline cellulose, UV ultraviolet, IR infra-red, NC nanocrystal, NIR near-infrared, PLA polylactide acid, PET Polyethylene terephthalate, MWIR mid-wave infrared, LWIR long-wave infrared, QD quantum dot.

Notes and references

1. L. Heux, G. Chauve, and C. Bonini, 2000, **07493**, 8210–8212.

2. S. Beck-Candanedo, M. Roman, and D. G. Gray, *Biomacromolecules*, 2005, **6**, 1048–54.

3. M. Roman and W. T. Winter, *Biomacromolecules*, 2004, **5**, 1671–7.

4. J. Araki and S. Kuga, 2001, 4493–4496.

5. D. Bondeson, A. Mathew, and K. Oksman, *Cellulose*, 2006, **13**, 171–180.

6. J. F. Revol, H. Bradford, J. Giasson, R. H. Marchessault, and D. G. Gray, *Int. J. Biol. Macromol.*, 1992, **14**, 170–2.

7. Y. Habibi, L. a Lucia, and O. J. Rojas, *Chem. Rev.*, 2010, **110**, 3479–500.

8. W. Hamad, 2006, **84**, 513–519.

9. B. L. Peng, N. Dhar, H. L. Liu, and K. C. Tam, *Can. J. Chem. Eng.*, 2011, **89**, 1191–1206.

10. H. Sehaqui, Z. Qi, O. Ikkala, and L. A. Berglund, *Biomacromolecules*, 2011.

11. M. A. Hubbe, O. J. Rojas, L. A. Lucia, M. Sain, and T. A. Forest, 2008, **3**, 929–980.

12. N. Durán, A. P. Lemes, and A. B. Seabra, *Recent Pat. Nanotechnol.*, 2012, **6**, 16–28.

13. A. Dufresne, *Molecules*, 2010, **15**, 4111–28.

14. A. Kaboorani, B. Riedl, P. Blanchet, M. Fellin, O. Hosseinaei, and S. Wang, *Eur. Polym. J.*, 2012, **48**, 1829–1837.

15. J. Iang, Z. Jiang, K. Ca, and R. Berry, 2011, **1**.

16. J. Han, C. Zhou, Y. Wu, F. Liu, and Q. Wu, *Biomacromolecules*, 2013, **14**, 1529–40.

17. R. Dash, Y. Li, and A. J. Ragauskas, *Carbohydr. Polym.*, 2012, **88**, 789–792.

18. J. P. F. Lagerwall, C. Schütz, M. Salajkova, J. Noh, J. Hyun Park, G. Scalia, and L. Bergström, *NPG Asia Mater.*, 2014, **6**, e80.

19. C. D. Edgar and D. G. Gray, 2001, 5–12.

20. H. Tang, B. Guo, H. Jiang, L. Xue, B. Li, X. Cao, Q. Zhang, and P. Li, *Cellulose*, 2013, **20**, 2667–2674.

21. J. Pan, W. Hamad, and S. K. Straus, *Macromolecules*, 2010, **43**, 3851–3858.

22. S. Belbekhouche, J. Bras, G. Siqueira, C. Chappey, L. Lebrun, B. Khelifi, S. Marais, and A. Dufresne, *Carbohydr. Polym.*, 2011, **83**, 1740–1748.

23. E. Borovitskaya and M. Shur, *Selective Topics in Electronics and Systems*, 2002.

24. R. F. Kazarinov and S. R.A, *Sov. Phys. Semicond*, 1971, **5**, 707.

25. A. Yoffe, *Adv. Phys.*, 2001, 1–208.

26. N. N. Ledentsov, V. M. Ustinov, V. a. Shchukin, P. S. Kop'ev, Z. I. Alferov, and D. Bimberg, *Semiconductors*, 1998, **32**, 343–365.

27. E. Biolatti, R. C. Iotti, P. Zanardi, and F. Rossi, *Phys. Rev. Lett.*, 2000, **85**, 5647–50.

28. a. Marent, M. Geller, a. Schliwa, D. Feise, K. Pötschke, D. Bimberg, N. Akçay, and N. Öncan, *Appl. Phys. Lett.*, 2007, **91**, 242109.

29. M. Gr, 2001, **414**.

30. I. Robel, V. Subramanian, M. Kuno, and P. V Kamat, *J. Am. Chem. Soc.*, 2006, **128**, 2385–93.

31. R. Turton, *The Quantum Dot: A Journey into the Future of Microelectronics*, 1996.

32. S. Coe, W. Wing-Keung, M. Bawendi, and V. Bulovic, *Nature*, 2002, **420**, 3–6.

33. V. L. Colvin, M. . Schlamp, and A. . Allvisatos, *Nature*, 1994, **370**, 354.

34. R. Ye, C. Xiang, J. Lin, Z. Peng, K. Huang, Z. Yan, N. P. Cook, E. L. G. Samuel, C.-C. Hwang, G. Ruan, G. Ceriotti, A.-R. O. Raji, A. A. Martí, and J. M. Tour, *Nat. Commun.*, 2013, **4**, 2943.

35. C. Cassidy, J. Kioseoglou, V. Singh, P. Grammatikopoulos, C. Lal, and M. Sowwan, *Appl. Phys. Lett.*, 2014, **104**, 161903.

36. N. Tessler, V. Medvedev, M. Kazes, S. Kan, and U. Banin, *Science*, 2002, **295**, 1506–8.

37. L. Levina, V. Sukhovatkin, S. Musikhin, S. Cauchi, R. Nisman, D. P. Bazett-Jones, and E. H. Sargent, *Adv. Mater.*, 2005, **17**, 1854–1857.

38. S. a McDonald, G. Konstantatos, S. Zhang, P. W. Cyr, E. J. D. Klem, L. Levina, and E. H. Sargent, *Nat. Mater.*, 2005, **4**, 138–42.

39. V. L. Colvin and A. N. Goldstein, 1992, **8721657**, 5221–5230.

40. M. Achermann, M. a Petruska, S. Kos, D. L. Smith, D. D. Koleske, and V. I. Klimov, *Nature*, 2004, **429**, 642–6.

41. D. Cahen, R. Naaman, and Z. Vager, *Adv. Funct. Mater.*, 2005, **15**, 1571–1578.

42. M. T. Neves-petersen, G. P. Gajula, and S. B. Petersen, 2011.

43. C. Turek and F. C. Stintzing, *Compr. Rev. Food Sci. Food Saf.*, 2013, **12**, 40–53.

44. E. Chiel, Y. Messika, S. Steinberg, and Y. Antignus, *Biocontrol*, 2006, **51**, 65–78.

45. N. Katsoulas, T. Bartzanas, C. Nikolaou, and C. Kittas, 2004.

46. Mears, R. David, J. R. William, and J. C. Simpkins, *Am. Soc. Agric. Eng.*, 1974, **NA74-112**.

47. D. Sridevi and K. V Rajendran, 2009, **32**, 165–168.

48. M. a. Gondal and M. a. Dastageer, *Appl. Phys. B*, 2011, **106**, 419–424.

49. X.-M. Chen, Y. Ji, X.-Y. Gao, and X.-W. Zhao, *Chinese Phys. B*, 2012, **21**, 116801.

50. J. Zhou, N. S. Xu, and Z. L. Wang, *Adv. Mater.*, 2006, **18**, 2432–2435.

51. X. Li, L. Wang, Y. Fan, Q. Feng, and F. Cui, *J. Nanomater.*, 2012, **2012**, 1–19.

52. J.-H. Park, L. Gu, G. von Maltzahn, E. Ruoslahti, S. N. Bhatia, and M. J. Sailor, *Nat. Mater.*, 2009, **8**, 331–6.

53. Y. Yin and a P. Alivisatos, *Nature*, 2005, **437**, 664–70.

54. R. M. Nielsen, S. Murphy, C. Strebel, M. Johansson, I. Chorkendorff, and J. H. Nielsen, *J. Nanoparticle Res.*, 2009, **12**, 1249–1262.

55. V. Srikant and D. R. Clarke, *J. Appl. Phys.*, 1998, **83**, 5447.

56. R. Yousefi, A. K. Zak, and F. Jamali-Sheini, *Ceram. Int.*, 2013, **39**, 1371–1377.

57. T. Huq, S. Salmieri, A. Khan, R. a Khan, C. Le Tien, B. Riedl, C. Fraschini, J. Bouchard, J. Uribe-Calderon, M. R. Kamal, and M. Lacroix, *Carbohydr. Polym.*, 2012, **90**, 1757–63.

58. S. Changes, O. F. Bamboo, and C. In, 2008, **3**, 297–315.

59. R. Kitamura, L. Pilon, and M. Jonasz, *Appl. Opt.*, 2007, **46**, 8118–33.